Robust, Parameter Insensitive Position Sensorless Field Orientation Control of the Induction Machine

C. J. Bonanno
Student Member, IEEE

Longya Xu
Senior Member, IEEE

The Ohio State University
Department of Electrical Engineering
2015 Neil Avenue
Columbus, Ohio 43210

Xingyi Xu
Member, IEEE

Ford Motor Company
Scientific Research Laboratory
P.O. Box 2053
Dearborn, Michigan 48121

Abstract: *A physcial approach is employed to estimate the rotor flux for a position sensorless induction machine drive system. This approach is based on the fundamental operating characteristics of the induction machine. The estimator structure calculates the rotor flux accurately at low speeds, and is largely insensitive to parameter variations. System structure, theoretical analysis, simulation, and laboratory results are presented.*

I. Introduction

Field Orientation Controlled (FOC) induction machine drives are used in industry where high precision performance is required. Application areas include the machine tool industry, robotics, steel and paper manufacturing, etc. Currently, research efforts are directed at establishing *position sensorless* FOC induction machine drives for applications where drives with encoders are not practical but high performance is essential. These areas include hazardous operating environments like the process control and chemical industries.

Many sensorless drives have been developed using different approaches. A physical approach was taken in [1], while more control oriented approaches were taken in [2],[3]. In [1], the authors presented a rotor flux oriented, position sensorless induction machine drive and showed that if the normal integration process is used to calculate the rotor flux, changing parameter values and low speed effects will result in an incorrect estimate. An inaccurate rotor flux estimate, in turn, produces an incorrect rotor speed estimate. The authors of [1] proposed a solution in which simple low pass filtering of both the back emf and flux command is done, resulting in a robust flux estimator which is largely insensitive to parameter variations and works well in a low speed range. In [2], the authors used the difference between two flux estimators and proposed a novel pole assignment method to realize a robust flux observer. This approach is more of a control oriented approach because of the use of Popov's criteria, linearization, and state-space pole assignment. There is less emphasis on machine physics, and how the machine physics affect rotor flux estimation. In [3], adaptive control theory is applied to synthesize an estimator. In addition, the estimator uses a parameter adaptive scheme to compensate for changing parameter values. For these reasons, we classify the approach in [3] as control oriented as well.

Two principle advantages exist in developing a drive using the approach of [1]. One, there is essentially no control system design needed to produce the flux estimator. No time is required to tune the estimator. For the physical approach, the critical information needed for implementation is the value of the rotor time constant. Two, the estimation algorithm is easily implemented in a DSP or dedicated hardware.

This paper clarifies the fundamental issues involved with a sensorless drive based on a frequency compensation scheme. This frequency compensation scheme forms the core of the physcial approach. The estimator explained in this paper, which uses the frequency compensation scheme, is a modified version of the estimator in [1].

Principles of rotor field orientation are presented, including an analysis of the frequency compensation scheme and speed estimation algorithm. Computer simulation results are then presented to demonstrate the success of the approach.

II. Rotor Field Orientation

A. Machine Model

The synchronous frame d-q induction machine model is shown in Figure 1. This model is oriented to the rotor flux. This means the sum of the expressions $M(i^e_{qs}+i^e_{qr})$ and $M(i^e_{ds}+i^e_{dr})$ yields the total flux linked by the rotor, respectively. Five equations are necessary to describe

0-7803-1859-5/94/$4.00

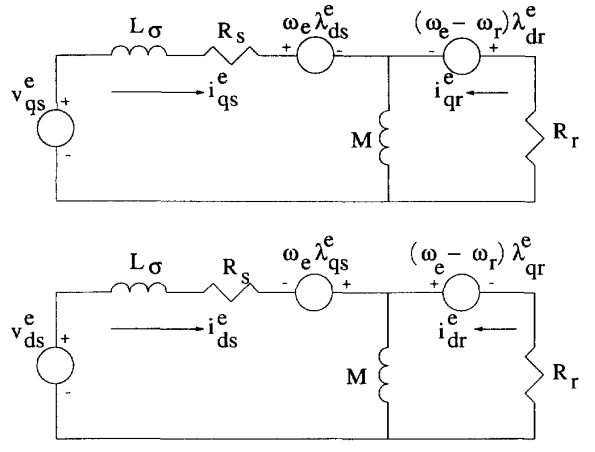

Figure 1: Rotor Flux d-q Model

a three phase symmetrical induction machine. The d-q equations of an induction machine oriented to the rotor flux are:

$$v_{qs}^e = L_\sigma \frac{di_{qs}^e}{dt} + R_s i_{qs}^e + \omega_e \lambda_{ds}^e + \frac{d\lambda_{qr}^e}{dt} \quad (1)$$

$$v_{ds}^e = L_\sigma \frac{di_{ds}^e}{dt} + R_s i_{ds}^e - \omega_e \lambda_{qs}^e + \frac{d\lambda_{dr}^e}{dt} \quad (2)$$

$$v_{qr}^e = R_r i_{qr}^e + (\omega_e - \omega_r)\lambda_{dr}^e + \frac{d\lambda_{qr}^e}{dt} \quad (3)$$

$$v_{dr}^e = R_r i_{dr}^e - (\omega_e - \omega_r)\lambda_{qr}^e + \frac{d\lambda_{dr}^e}{dt} \quad (4)$$

$$T_e = J\frac{d\omega_{rm}}{dt} + B_m\omega_{rm} + T_l \quad (5)$$

where

$$\lambda_{qr}^e = M(i_{qs}^e + i_{qr}^e) \quad (6)$$

$$\lambda_{dr}^e = M(i_{ds}^e + i_{dr}^e) \quad (7)$$

$$T_e = \frac{3P}{4}(\lambda_{dr}^e i_{qs}^e - \lambda_{qr}^e i_{ds}^e) \quad (8)$$

The first principle of field orientation is to align the rotor flux with the d axis. This forces $\lambda_{qr}^e = 0$. The conditions for field orientation control are derived from the rotor voltage and rotor flux equations listed above, with the condition $\lambda_{qr}^e = 0$. Equations (3) (4) (6) (7) and (8) are listed in reduced form:

$$(\omega_e - \omega_r) = \frac{-R_r i_{qr}^e}{\lambda_{dr}^e} \quad (9)$$

$$\frac{d\lambda_{dr}^e}{dt} = -R_r i_{dr}^e \quad (10)$$

$$i_{qs}^e = -i_{qr}^e \quad (11)$$

$$\lambda_{dr}^e = M(i_{ds}^e + i_{dr}^e) \quad (12)$$

$$T_e = \frac{3P}{4}(\lambda_{dr}^e i_{qs}^e) \quad (13)$$

The slip condition is found by inserting (11) into (9);

$$\omega_e - \omega_r = s\omega_e = \frac{R_r i_{qs}^e}{\lambda_{dr}^e} \quad (14)$$

From Equation (12),

$$i_{dr}^e = \frac{\lambda_{dr}^e}{M} - i_{ds}^e \quad (15)$$

The flux condition is found by inserting (15) into (10);

$$\lambda_{dr}^e = \frac{M i_{ds}^e}{1 + T_r p} \quad (16)$$

where T_r is the rotor time constant and is equal to

$$T_r = \frac{M}{R_r} \quad (17)$$

B. *Rotor Flux Estimation Scheme*

The stationary frame *vector* model of the rotor flux oriented induction machine is shown in Figure 2. This model is chosen because it is the basis for rotor flux estimation. The block diagram of the proposed rotor flux estimator is shown in Figure 3.

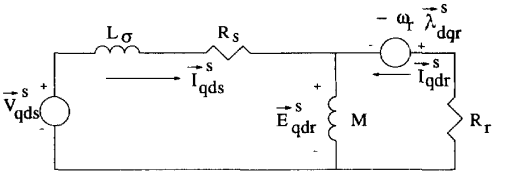

Figure 2: Vector Model in Stationary Frame

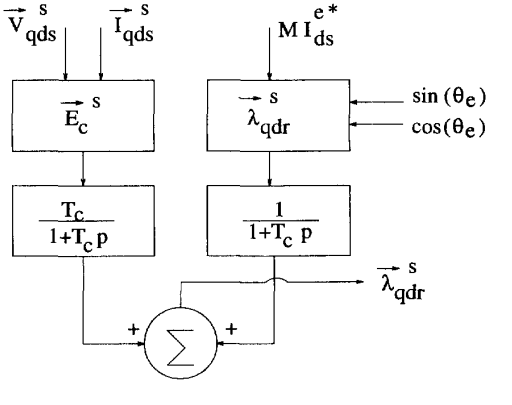

Figure 3: Flux Estimator Block Diagram

Note that the block diagram realizes the rotor flux estimator according to the following equation:

$$\vec{\lambda}^s_{qdr} = \frac{T_c \vec{E}^s_c}{1+T_c p} + \frac{\vec{\lambda}^{s^*}_{qdr}}{1+T_c p} \tag{18}$$

The frequency domain version of (18) is:

$$\vec{\lambda}^s_{qdr} = \frac{T_c \vec{E}^s_c}{1+j\omega_e T_c} + \frac{\vec{\lambda}^{s^*}_{qdr}}{1+j\omega_e T_c} \tag{19}$$

where the vectors are defined as:

$$\vec{\lambda}^{s^*}_{qdr} = \begin{bmatrix} \lambda^{s^*}_{qr} \\ \lambda^{s^*}_{dr} \end{bmatrix} \vec{E}^s_c = \begin{bmatrix} E^s_{cqr} \\ E^s_{cdr} \end{bmatrix} \vec{\lambda}^s_{qdr} = \begin{bmatrix} \lambda^s_{qr} \\ \lambda^s_{dr} \end{bmatrix} \tag{20}$$

Using the stator voltages and currents, the calculated back emf, $\vec{E}^s_c$, is given by:

$$\vec{E}^s_c = \vec{V}^s_{qds} - (R^*_s + j\omega_e L^*_\sigma)\vec{I}^s_{qds} \tag{21}$$

where R^*_s and L^*_σ are the nominal values of stator resistance and leakage inductance. The nominal values are related to the actual values by:

$$R^*_s = R_s - \Delta R_s \tag{22}$$

$$L^*_\sigma = L_\sigma - \Delta L_\sigma \tag{23}$$

Inserting (22) and (23) into (21) yields:

$$\vec{E}^s_c = \vec{V}^s_{qds} - ((R_s - \Delta R_s) + j\omega_e(L_\sigma - \Delta L_\sigma))\vec{I}^s_{qds} \tag{24}$$

According to Figure 2, the actual back emf, $\vec{E}^s_{qdr}$, is

$$\vec{E}^s_{qdr} = \vec{V}^s_{qds} - (R_s + j\omega_e L_\sigma)\vec{I}^s_{qds} \tag{25}$$

Therefore, the calculated and actual back emfs are related by

$$\vec{E}^s_c = \vec{E}^s_{qdr} + (\Delta R_s + j\omega_e \Delta L_\sigma)\vec{I}^s_{qds} \tag{26}$$

For notation purposes, the following expressions are introduced:

$$\vec{\mu} = \frac{1}{1+j\omega_e T_c} = |\vec{\mu}|\,\angle\phi \tag{27}$$

where

$$|\vec{\mu}| = \frac{1}{\sqrt{1+(\omega_e T_c)^2}} \quad \text{and} \quad \angle\phi = -tan^{-1}(\omega_e T_c) \tag{28}$$

Then, the estimated flux expressed in (19) becomes:

$$\vec{\lambda}^s_{qdr} = \vec{\mu}\, T_c\, \vec{E}^s_c + \vec{\mu}\, \vec{\lambda}^{s^*}_{qdr} \tag{29}$$

The torque current i^e_{qs} in the synchronous reference frame is estimated from the stationary flux components by:

$$i^e_{qs} = \frac{i^s_{qs}\lambda^s_{dr} - i^s_{ds}\lambda^s_{qr}}{\sqrt{(\lambda^s_{dr})^2 + (\lambda^s_{qr})^2}} \tag{30}$$

C. *Speed Estimation Scheme*

The slip speed and synchronous speed can be calculated from the estimated rotor flux. It follows that the estimated rotor speed is the difference between the synchronous and slip speeds. The slip speed $s\omega_e$ in a rotor flux oriented drive is *uniquely* determined by the torque current i^e_{qs} and rotor flux magnitude $|\lambda^e_{dr}|$,

$$s\,\omega_e = \frac{R_r\, i^e_{qs}}{|\lambda^e_{dr}|} \tag{31}$$

with i^e_{qs} obtained from Equation (30), and the magnitude of the rotor flux obtained through:

$$|\lambda^e_{dr}| = \sqrt{(\lambda^s_{dr})^2 + (\lambda^s_{qr})^2} \tag{32}$$

The synchronous speed is also estimated from the rotor flux:

$$\omega_e = \frac{d\theta_e}{dt} \quad \text{and} \quad \theta_e = tan^{-1}\left(\frac{\lambda^s_{qr}}{\lambda^s_{dr}}\right) \tag{33}$$

$$\omega_e = \frac{\lambda^{s'}_{qr}\lambda^s_{dr} - \lambda^s_{qr}\lambda^{s'}_{dr}}{(\lambda^s_{dr})^2 + (\lambda^s_{qr})^2} \tag{34}$$

The rotor speed, therefore, is

$$\omega_{rm} = \omega_e - s\,\omega_e \tag{35}$$

D. *Parameter Sensitivity and Low Speed Effects*

In order to investigate the parameter sensitivity and low speed effects of the proposed estimation scheme, Equations (26) and (29) are combined to form:

$$\vec{\lambda}^s_{qdr} = \vec{\mu}\, T_c(\vec{E}^s_{qdr} + (\Delta R_s + j\omega_e \Delta L_\sigma)\, \vec{I}^s_{qds}) + \vec{\mu}\, \vec{\lambda}^{s^*}_{qdr} \tag{36}$$

Let

$$\vec{\lambda}^s_{qdr} = \vec{\lambda}_1 + \vec{\lambda}_2 + \vec{\lambda}_3 \tag{37}$$

Then

$$\vec{\lambda}_1 = \vec{\mu}\, T_c\, \vec{E}^s_{qdr} \tag{38}$$

$$\vec{\lambda}_2 = \vec{\mu}\, T_c\, (\Delta R_s + j\omega_e \Delta L_\sigma)\, \vec{I}^s_{qds} \tag{39}$$

$$\vec{\lambda}_3 = \vec{\mu}\, \vec{\lambda}^{s^*}_{qdr} \tag{40}$$

1. Parameter Sensitivity

It is observed that only $\vec{\lambda}_2$ is subjected to parameter variations, and thus the robustness of the estimator will improve if $\vec{\lambda}_2$ is negligibly small. The vector $\vec{\lambda}_2$ can be made to approximate zero by a proper selection of T_c, the filter time constant. To examine this, Equation (39) is re-written as:

$$\vec{\lambda}_2 = \vec{\mu}\, T_c\, \Delta Z\, \angle\gamma\, \vec{I}^s_{qds} \tag{41}$$

where

$$\Delta Z = \sqrt{\Delta R_s{}^2 + (\omega_e \Delta L_\sigma)^2} \tag{42}$$

and

$$\gamma = tan^{-1}(\frac{\omega_e \Delta L_\sigma}{\Delta R_s}) \tag{43}$$

Equation (41) can also be expressed as:

$$\vec{\lambda}_2 = T_c|\vec{\mu}|\Delta Z \angle(\phi + \gamma)\vec{I}^s_{qds} \tag{44}$$

Setting $\phi + \gamma = 0$,

$$tan^{-1}(\omega_e T_c) = tan^{-1}(\frac{\omega_e \Delta L_\sigma}{\Delta R_s}) \tag{45}$$

This requires that

$$T_c = \frac{\Delta L_\sigma}{\Delta R_s} \tag{46}$$

Note that

$$\frac{\Delta L_\sigma}{\Delta R_s} \doteq \frac{M}{R_r} \tag{47}$$

Thus, by choosing

$$T_c = \frac{M}{R_r} \tag{48}$$

which is exactly the rotor time constant, the phase of $\vec{\lambda}_2$ will be approximately zero. Likewise,

$$\Delta Z|\vec{\mu}| = 1 \tag{49}$$

Equation (44) can be written as:

$$\vec{\lambda}_2 = T_c \vec{I}^s_{qds} \tag{50}$$

As indicated, parameter sensitivity is minimized by minimizing $\vec{\lambda}_2$ in terms of both magnitude and phase angle.

2. Low Speed Effects

The performance improvement of the flux estimator is explained by examining $\vec{\lambda}_1$ and $\vec{\lambda}_3$ only, since $\vec{\lambda}_2$ is negligibly small. In a low speed range, $\vec{\lambda}_1$ will not be orthogonal to the back emf. The vector $\vec{\lambda}_3$ drives the vector $\vec{\lambda}_1$ to the correct position. Re-writing Equation (40) as:

$$\vec{\lambda}_3 = \frac{1}{\omega_e(\sqrt{1 + (\omega_e T_c)^2})} \angle(\phi - 90^o)\vec{E}^{s*}_{qdr} \tag{51}$$

and letting

$$\vec{E}^s_{qdr} = \vec{E}^{s*}_{qdr} \tag{52}$$

$\vec{\lambda}^s_{qdr}$ can be written:

$$\vec{\lambda}^s_{qdr} = |\vec{\mu}|\left(T_c \angle\phi + \frac{1}{\omega_e}\angle(\phi - 90^o)\right)\vec{E}^s_{qdr} \tag{53}$$

Examining Equation (53), $\vec{\lambda}_3$ adds the necessary amount of phase to make the back emf and flux orthongonal in a low speed range, and thus is the *compensating* component of the flux estimator.

A phasor diagram was constructed in Figure 4 to graphically illustrate how the components of the flux estimator are related. At low speeds, $\vec{\lambda}_1$ is not sufficiently shifted to be orthongonal to $\vec{E}^s_c$, such that the addition of $\vec{\lambda}_3$ will bring $\vec{\lambda}_1$ to its correct position. Also, as λ_2 approaches to zero, the sum of $\vec{\lambda}_2$ and $\vec{\lambda}_1$ approaches $\vec{\lambda}_1$, and the phase error due to the resistive parameters is reduced to a low level. Conversely, at high speeds $\vec{\lambda}_1$ is orthogonal to $\vec{E}^s_{qdr}$ and the magnitude of $\vec{\lambda}_3$ is quite small. In essence, the phase contribution of $\vec{\lambda}_3$ to $\vec{\lambda}_1$ is naturally reduced in a high speed range due to the low pass filter.

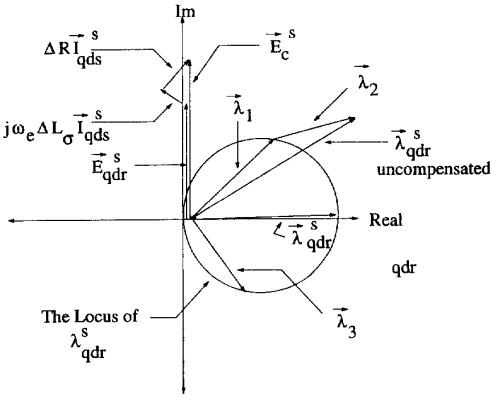

Figure 4: Phasor Diagram of Flux Estimator

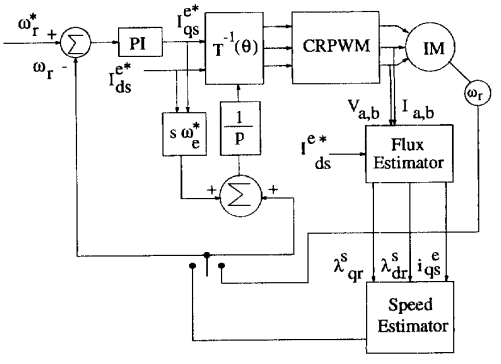

Figure 5: System Block Diagram for Computer Simulation

III. Computer Simulation Results

A computer simulation was conducted of the system shown in Figure 5 to evaluate the performance of the estimator. The machine simulated has specifications listed in Table 1. In the simulation, the speed was initially stabilized at 150 rpm and then ramped down to 75 rpm. The low speed range was selected to examine any differences between the uncompensated and compensated flux with respect to the real flux.

In case 1, no parameter variation is assumed. Simulation results are shown in Figures 6 & 7.

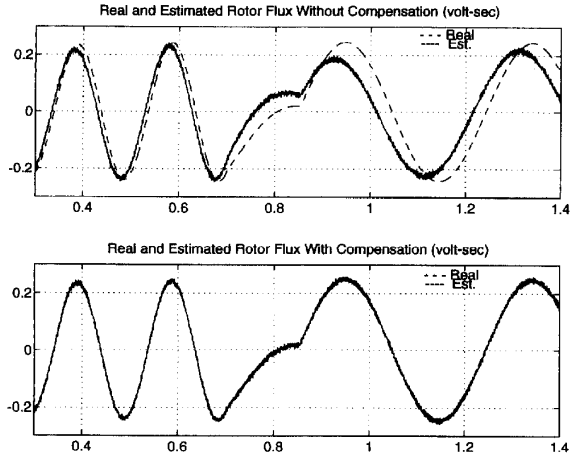

Figure 6: Rotor Flux: No Parameter Variation

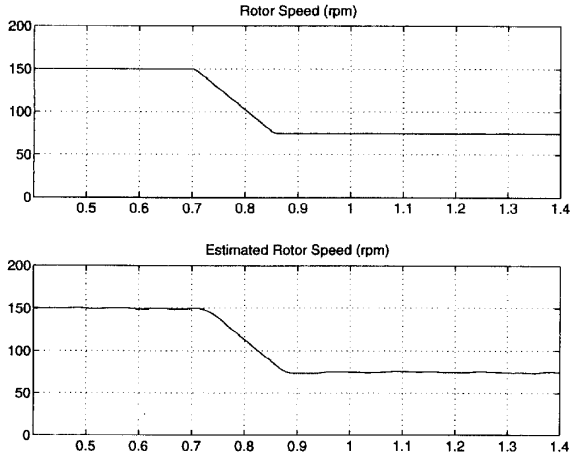

Figure 7: Rotor Speed: No Parameter Variation

It is evident that without compensation ($\vec{\lambda}_3 = 0$), the error of the estimated rotor flux is substantial. With compensation, the accuracy of the rotor flux is much improved even at $\omega_{rm} = 75$ rpm.

To verify the robustness of the estimator in case 2, the stator resistance was changed 12 % over 1.7 seconds. The compensated flux is still accurate, and there is little difference between the real and estimated flux, as shown in Figures 8 & 9.

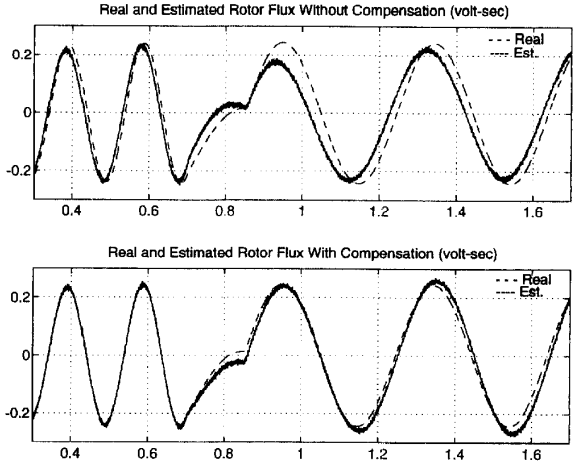

Figure 8: Rotor Flux: Parameter Variation

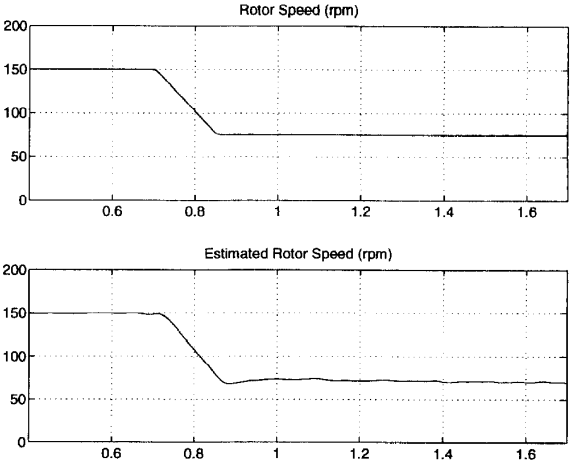

Figure 9: Rotor Speed: Parameter Variation

The third case consists of closed speed loop regulation. The tachometer in Figure 5 is disconnected and the estimated speed is used for speed regulation and determination of θ_e. The results are shown in Figures 10 and 11.

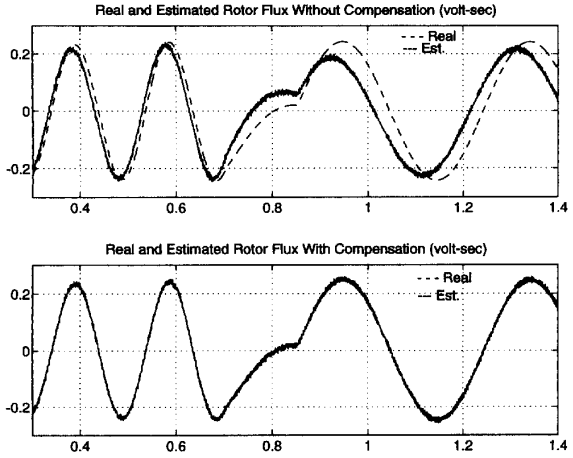

Figure 10: Rotor Flux: Closed Speed Loop Regulation

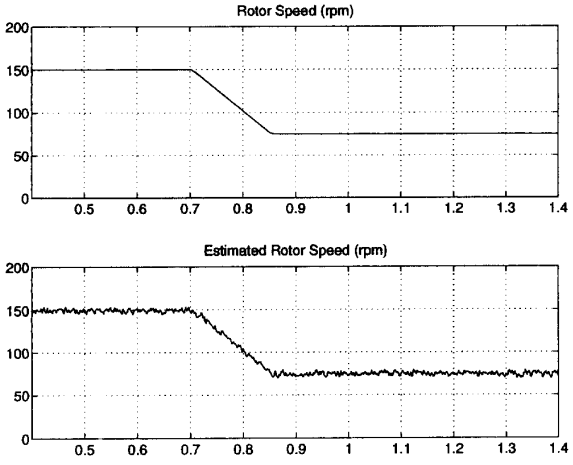

Figure 11: Rotor Speed: Closed Speed Loop Regulation

The results show that closed loop speed regulation is obtained satisfactorily using the flux and speed estimator described previously.

Table1

220 Volts	15 Amps	5 HP
$L_\sigma = 4$ mH	$M = 35.2$ mH	1800 rpm
$R_s = 1.1\,\Omega$	$R_r = .2696\,\Omega$	4 poles

IV. Conclusions

A physical approach is presented for a position sensorless, field orientation controlled induction machine drive system. The key issue in a position sensorless drive is to observe the rotor flux correctly. Then the rotor speed can be calculated accurately. For the physical approach, the rotor flux is estimated accurately by making the rotor flux and back emf orthogonal even in a low speed range and subject to parameter variations. The algorithm simplicity is an attractive feature for implementation on a DSP real time control system.

The position sensorless drive explained in this paper is being implemented in the Power Electronics Laboratory at Ohio State University. Experimental results will be presented in the near future.

V. References

[1] T. Ohtani, N. Takada, and K. Tanaka, "Vector Control of Induction Motor Without Shaft Encoder," in *Proceedings of the IEEE-IAS Annual Conference,* 1989, pages 500-507.

[2] H.Tajima, Y. Hori, "Speed Sensorless Field-Orientation Control of the Induction Machine," *IEEE-IAS Transactions,* Vol. 29, No. 1, pages 175-180, January-February 1993.

[3] Kubota, H., Matsuse, K., and Nakano, T., "DSP-Based Speed Adaptive Flux Observer of Induction Motor," *IEEE-IAS Transactions,* Vol. 29,No. 2, pages 344-348, March-April 1993.

[4] X. Xu, R. De Doncker, and D. Novotny, "Implementation of Direct Stator Flux Orientation Control on a Versatile DSP Based System," *Proceedings of the IEEE-IAS Annual Conference,"* 1990, pages 404-409.

[5] X. Xu, and D. Novotny, "Selection of the Flux Reference for Induction Machine Drives in the Field Weakening Region," *IEEE-IAS Transactions,* Volume 28, No. 6, pages 1353-1358, November/December 1992.

[6] F.Z. Peng, and T. Fukao, "Robust Speed Identification for Speed Sensorless Vector Control of Induction Motors," *Proceedings of the IEEE-IAS Annual Conference,* 1993, pages 419-426.

[7] P.L. Jansen, R.D. Lorenz, and D.W. Novotny, "Observer-Based Field Orientation Analysis and Comparison of Alternative Methods," *Proceedings of the IEEE-IAS Annual Conference,* 1993, pages 536-543.